



Optimal switching renewable energy system for demand side management

Zhou Wu^{*}, Xiaohua Xia

Department of Electrical Electronic and Computer Engineering, University of Pretoria, Pretoria, South Africa

Received 5 December 2014; received in revised form 28 January 2015; accepted 1 February 2015

Communicated by: Associate Editor Mukund R. Patel

Abstract

Renewable hybrid systems with small capacities are widely installed for joining demand response in modern communities. Based on hybrid systems, renewable energy generation can be stored and used for power supply during peak load period. It is impractical to control power flow in such small-scale systems, because power flow dispatching asks for extra investment of expensive regulators and adaptors. In this paper, a switching grid connected photovoltaic system is studied for simplifying system installation. Optimal switching control model is proposed to sufficiently utilize the solar energy and to minimize electricity cost under the time-of-use program. As shown in results, optimal scheduling of the PV system can achieve promising cost savings.

© 2015 Elsevier Ltd. All rights reserved.

Keywords: Optimal switching control; Solar energy; Renewable energy; Distributed generation; Demand side management

1. Introduction

Due to globally increasing energy consumption, fossil fuel resources suffer from risks of over exploration and possible distinction in the near future. Meanwhile carbon and pollutant emissions caused by burning of fossil fuel have been growing over the last decade with great threat to environment (Wu et al., 2015). To control fossil fuel consumption and carbon emissions, exploration of new clean energy resources is necessary to decelerate the increasing rate of fuel consumption and reduce it if possible. Renewable energy (RE) resources have become an increasingly significant part of power generation for reducing fossil fuel consumption and pollutant emission (Esen and Yuksel, 2013). Among available RE technologies, wind and solar energy

sources are the most promising options, as they are omnipresent, freely available, and environmental friendly.

Wind and solar generators usually require storage components (battery, ultra-capacitor, and so on) due to their drawback of intermittent nature. Combination of multiple power sources and storage components can provide a stable power supplier, which is the so-called renewable hybrid system. One common application of hybrid systems is the installation in remote areas for stand-alone supply (Nema et al., 2009; Shaahid and El-Amin, 2009). Especially, the photovoltaic (PV) systems are widespread due to universal availability of solar energy. Researchers have great interests on stand-alone or grid connected PV systems, including various topics like PV sizing (Arun et al., 2009), scheduling (Gabash and Li, 2013; Kanchev et al., 2011), and maximum power point tracking (MPPT) (Soto et al., 2006).

Life cycle cost and power generation efficiency are two main criteria to evaluate performance of exploring

^{*} Corresponding author.

E-mail addresses: wuzhsky@gmail.com (Z. Wu), xxia@up.ac.za (X. Xia).

Nomenclature

$P_1(t)$	power flow from the diesel generator to the load at time t (kW)	$u_2(t)$	status of switch on the line connecting the grid and the battery charger at time t
$P_2(t)$	power flow from the PV to the load at time t (kW)	$u_3(t)$	status of switch on the line connecting the battery inverter and the load at time t
$P_3(t)$	power flow from the PV array to the load at time t (kW)	$u_4(t)$	status of switch on the line connecting the grid and the load at time t
$P_4(t)$	power flow from the battery to the load at time t (kW)	$u_5(t)$	status of switch on the line connecting the PV and the load at time t
$P_{pv}(t)$	power output from the PV generator at time t (kW)	$S(t)$	the state of charge (SOC) of battery (kW)
$P_L(t)$	load demand at time t (kW)	S^{max}	the maximum capacity of battery (kW)
$P_G(t)$	power output from the grid to the battery at time t (kW)	S^{min}	the allowable minimum SOC of battery (kW)
$u_1(t)$	status of switch on the line connecting the PV and the battery charger at time t	DoD	the depth of discharge
		η_C	the charging efficiency of battery
		η_D	the discharging efficiency of battery
		$\rho(t)$	the price of electricity (\$/kW h)

renewable energy (Shaahid and El-Amin, 2009; Wies et al., 2005; Esen et al., 2006; Esen et al., 2007). Simulation model for economic analysis and environmental impacts is proposed for a PV–diesel–battery (PDB) system (Wies et al., 2005), in which the fuel cost is calculated over a one-year period and simple payback is evaluated. The PDB hybrid system is proven with ability of reducing the operation costs and the emission of greenhouse gases. In Tazvinga et al. (2013), daily energy consumption variations between winter and summer are considered into scheduling the PDB system. The authors have evaluated operational efficiency of the hybrid system over a 24-h period and optimal solutions can be found to reduce the corresponding fuel costs. Their conclusion is that 73–77% fuel savings in winter and 80.5–82% fuel savings in summer can be achieved by the optimal control method. In Tazvinga et al. (in press), two objectives of fuel cost and battery wear cost have been considered in the optimal management of the PDB hybrid system.

Nowadays, a rising number of individuals take part in demand response (DR) programs, such as peak shaving, load shifting, power reduction and time-of-use (TOU) (Aalami et al., 2010). Small-capacity hybrid systems installed in more families or small communities can play significant roles in demand side management (DSM). On the other hand, some remote areas, where customers used to rely on stand-alone hybrid systems for supplying power, are getting connection to the grid as part of network upgrade. The installed hybrid system is necessarily modified to earn benefits in DSM. For controlling such hybrid systems, some rule-based strategies about power flow dispatching (Wang and Nehrir, 2008; Jain and Agarwal, 2008; Teleke et al., 2010) can obtain promising but not optimal solutions that can ensure practical constraints

satisfied. Optimal control is a useful method to schedule power flows of hybrid systems with minimum cost and maximum benefit (Tazvinga et al., 2013; Riffonneau et al., 2011; Tazvinga et al., 2014). However, power flow control is impractical for small-capacity hybrid systems that have been widely equipped individually, because power control asks for extra investment of expensive regulators and adaptors. Therefore, a simple but practical switching model of grid connected PV system with storage is proposed at demand side. The scheduling of the PV system for DSM is based on an optimal switching control approach. To our best knowledge, few works emphasize on optimal switching control of hybrid system to reduce the power consumption and the electricity cost at demand side. In this paper, the optimal switching control will be studied for the grid-connected PV system in the framework of TOU, in which the electricity price is high in the peak hours and is low in the off-peak hours (Aalami et al., 2010). As the electricity prices are fixed in advance for the customer reference, day-ahead optimal switching control is applicable to minimize the electricity cost under the TOU program.

The main contributions of this work include three aspects. Firstly, a switching model of the grid connected PV system with storage is proposed with simple structure. The PV system can be newly installed or modified from other existing hybrid systems with low construction cost. Secondly, the PV system is analyzed in the viewpoint of control system theory. System state-space equations are deduced, and optimal control is proposed to schedule the PV system for DSM. Thirdly, the optimal control approach can minimize the electricity cost and ensure all practical constraints satisfied. The performance of optimal control is better than an intuitive control method.

This paper is organized as follows. A commonly used PDB hybrid system is introduced and its power flow control methods are reviewed in Section 2. A grid-connected PV system with storage is modeled in Section 3. An optimal switching control approach is proposed to minimize the electricity cost at demand side in Section 4. Then optimal control is developed as the open-loop control to stably and economically operate switches of the PV system. The results of optimal switching control are presented in Section 5. Discussions of parameter variation are given in Section 6, while the conclusion section is Section 7.

2. Original PV–diesel–battery hybrid system

The original PDB system studied in Tazvinga et al. (2013), Tazvinga et al. (in press), Tazvinga et al. (2014), Zhu et al. (2014) is made up of three main subsystems, i.e., the PV generation, the battery storage and the diesel generation (DG), as shown in Fig. 1. The load is initially met by the PV generation and then the battery comes in when the PV output is not enough to meet the load. Only when both the PV and battery cannot meet the load, the diesel eventually comes in because the diesel consumption is costly. The battery is charged when the PV output has surplus after satisfying the load demand. In the schematic of PDB hybrid system, control variables P_1 , P_2 and P_4 represent the power flows from the DG, PV, and battery to the load respectively and P_3 represents the power flow from the PV to the battery. The subsystems are introduced as follows, which can be referred from Tazvinga et al. (2013) and Tazvinga et al. (2014).

2.1. PV array

Each solar array consists of several solar cells to convert solar irradiation into direct current power. The hourly power output of PV arrays with a given size can be simply formulated as:

$$P_{pv} = \eta_{pv} I_{pv} A_c, \quad (1)$$

where P_{pv} is the hourly power output from PV arrays; η_{pv} is the efficiency of solar generation; I_{pv} is the hourly solar irradiation incident on the PV array (kW h/m^2); A_c is the size of PV arrays.

The hourly solar irradiation incident on the PV array has complicated relations with time of a day, season of a year, tilt, location, global irradiation, and diffuse fraction.

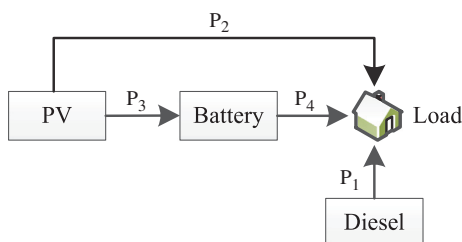


Fig. 1. Schematic of the PDB hybrid system.

In this study, the simplified isotropic diffuse formula (Tazvinga et al., 2013; Collares-Pereira and Rabl, 1979) is used as

$$I_{pv} = (I_B + I_D)R_B + I_D, \quad (2)$$

where I_B is the beam component of the hourly global irradiation and I_D is the hourly diffuse irradiation respectively. R_B is a geometric ratio of the actual irradiation on the tilted plane to the standard irradiation on the horizontal plane.

The efficiency of solar generation can be expressed as a function of the hourly irradiation I_{pv} and the ambient temperature T_A as

$$\eta_{pv} = \eta_R \left[1 - \frac{0.9\beta I_{pv}(T_{C0} - T_{A0})}{I_{pv0}} - \beta(T_A - T_R) \right], \quad (3)$$

where η_R is the PV generation efficiency that is measured at the referenced cell temperature T_R (25°C); β is the temperature coefficient for cell efficiency (typically 0.004 – $0.005/^\circ\text{C}$); T_{C0} (typically 45°C) and T_{A0} (typically 20°C) are the cell and ambient temperatures at the nominal operating cell temperature (NOCT) test; I_{pv0} is the average solar irradiation on the array at the NOCT test.

2.2. Battery bank

Being constrained in battery capacity, the state of charge (SOC) changes dynamically owing to possible charge by the PV and grid or possible discharge for customer usage. For a given profile of power generation, customers' demand will mostly affect the SOC of battery. Let t denote time of day (the system is sampled in every hour in this paper), and $S(t)$ denote the SOC of battery at the t th hour. Based on the current SOC, the dynamic change of SOC at the next hour can be formulated as

$$S(t+1) = S(t) + \eta_C P_3(t) - \frac{P_4(t)}{\eta_D}, \quad (4)$$

where $P_3(t)$ is the grid power for charging the battery over $[t, t+1)$; $P_4(t)$ is the power discharged from the battery over $[t, t+1)$. $\eta_C \leq 1$ and $\eta_D \leq 1$ are the coefficients of charging and discharging efficiency respectively. According to Eq. (4), the current SOC $S(t)$ can be expressed by the initial SOC $S(0)$ of a day as

$$S(t) = S(0) + \eta_C \sum_{\tau=0}^{t-1} P_3(\tau) - \frac{1}{\eta_D} \sum_{\tau=0}^{t-1} P_4(\tau). \quad (5)$$

The SOC of battery has several constraints, such as the allowable maximum capacity and the depth of discharge (DoD). The lower bound of SOC S^{min} can be expressed by the DoD as

$$S^{min} = (1 - \text{DoD})S^{max}, \quad (6)$$

where DoD is the depth of discharge; S^{max} is the maximum capacity of the battery; S^{min} is the allowable minimum SOC of the battery. The SOC must be bounded within the scale $[S^{min}, S^{max}]$.

2.3. Diesel generator

DG is incorporated in the PDB hybrid system as backup resource to cover the power deficiency that the PV and battery cannot provide. The fuel consumption of DG (Tazvinga et al., 2013; Penangsang et al., 2014) can be formulated as

$$V(t) = aP_1^2(t) + bP_1(t), \quad (7)$$

where $P_1(t)$ is the power output of DG over $[t, t + 1)$; $V(t)$ is the volume of diesel consumed over $[t, t + 1)$ (L); a and b are fuel consumption coefficients. DG power has to be restricted between the rated power and specified minimum value as

$$P_1^{min} \leq P_1(t) \leq P_1^{max}, \quad (8)$$

where P_1^{max} is the rated power and P_1^{min} is the minimum power requirement.

2.4. Power flow control methods

In Tazvinga et al. (2013), an optimal power flow dispatch model is built to determine the optimal schedule of the PDB hybrid system for minimizing the fuel cost. The power flows are constrained by the demand balance, PV output and operational limits. The objective function and constraints are given as

$$\begin{aligned} \min C_f \sum_{t=0}^{T-1} [aP_1^2(t) + bP_1(t)], \\ \text{s.t.} \begin{cases} P_i^{min} \leq P_i(t) \leq P_i^{max} \\ P_2(t) + P_3(t) \leq P_{pv}(t) \\ P_1(t) + P_2(t) + P_4(t) = P_L(t) \\ S^{min} \leq S(t) \leq S^{max} \end{cases} \end{aligned} \quad (9)$$

where $0 \leq t < T$ and T is the evaluation period and C_f is the fuel price (\$/L).

In Tazvinga et al. (in press), an optimal power flow control model is proposed to minimize both fuel cost and battery wear cost in the PDB hybrid system while the practical constraints, such as the load balance and battery SOC limits, are satisfied. Using the weighted sum method, these two objectives can be integrated into a single function given as

$$\min w_1 C_f \sum_{t=0}^{T-1} [aP_1^2(t) + bP_1(t)] + w_2 C_{bw} \sum_{t=0}^{T-1} [P_3(t) + P_4(t)] \quad (10)$$

where w_1 and w_2 are weights satisfying $w_1 + w_2 = 1$; C_{bw} is the battery wear cost per unit of power input and output. In this model, the constraints of Eq. (10) are the same as those in Eq. (9).

3. Model of grid connected PV system

The grid connected PV system with battery backup evaluated in this paper consists of PV arrays and battery

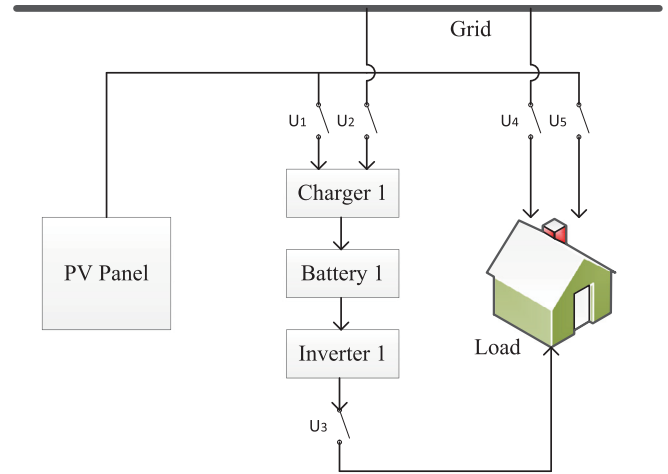


Fig. 2. Schematic of the switching PV system.

bank that are connected to the grid as shown in Fig. 2. Note that the PDB hybrid system in Fig. 1 was originally installed for stand-alone power supply at the target region (Tazvinga et al., 2013; Zhu et al., 2014). Due to enlarged coverage of grid, the target region has connection with grid. Now a new problem is how to use such installed small scale system efficiently with grid connection. As a modification of the PDB hybrid system, the switching PV system with storage is proposed to solve this problem in necessity. The proposed system will be modeled in this section.

3.1. Description of the PV system

The PV system studied in this paper is called a switching system as each power line is equipped with a controllable switch, such as relay or metal–oxide–semiconductor field-effect transistor (MOSFET). In the switching hybrid system, chargers and inverters are required for voltage and current matching, such as direct current (DC)/alternating current (AC) and DC/DC. Each power line is controlled by a switch and arrows in the figure represent directions of power flows on power lines. The battery is connected with the PV arrays and the grid, and the load is connected with the battery, PV and grid for satisfying demand.

Compared with the PDB hybrid system (Tazvinga et al., 2013; Zhu et al., 2014), the diesel generator has been excluded in the grid connected PV system, because buying electricity from grid is cheaper and greener than consuming diesel for power generation. Unlike the PDB system, in which additional adaptors or regulators are required to dispatch designed power flow on each line, the switching PV system has a simply structure that does not require these costly components. For the switching system, only one power resource is allowed to provide the demand power, and only one power resource is allowed to charge the battery. Meanwhile, the battery is not allowed for charging and discharging simultaneously. However, the switching system can achieve the same functions, i.e., continuous power supply, solar energy usage and storage, and electricity cost saving.

3.2. DSM of the PV system

Nowadays DSM has been widely used in the electricity market, and renewable hybrid systems play increasingly significant roles in demand side management. In this paper, TOU program is considered as a typical DR program for studying the PV system at demand side. In TOU, the electricity price changes over different periods according to the electricity supply cost. For example high price is paid for peak load periods, medium price is paid for standard periods and low price is paid for off-peak periods. In this study, the electricity price at the target region can be given as

$$\rho(t) = \begin{cases} \rho_k, & t \in [7, 10) \cup [18, 20), \\ \rho_o, & t \in [0, 6) \cup [22, 24), \\ \rho_s, & t \in [6, 7) \cup [10, 18) \cup [20, 22), \end{cases} \quad (11)$$

where $\rho_k = 0.20538$ \$/kWh is the price of peak load period; $\rho_o = 0.03558$ \$/kWh is the price of off-peak period; $\rho_s = 0.05948$ \$/kWh is the price of standard period. Without the PV system, the electricity cost over the period $[0, T)$ is $\int_{\tau=0}^T \rho(\tau)P_L(\tau)d\tau$.

In the viewpoint of DSM using the PV system, the battery can be charged by the grid in the off-peak period, and then discharged in the peak period to reduce electricity cost. The grid can also provide electricity directly when the customer demand cannot be satisfied by the battery. The model of switching PV system is built to formulate the electricity cost under certain switching strategies.

3.3. SOC dynamic of switching system

In the grid-connected PV system, the battery SOC is increasing over time due to charge of the PV and grid, and the battery SOC is decreasing over time due to discharge for the customer usage. As shown in Fig. 2, if U_1 or U_2 is switching on the battery is charging by the PV or grid; if U_3 is switching on the battery is discharged for satisfying the load demand. Given the current SOC at the t th hour, the SOC of the next hour can be formulated as

$$S(t+1) = S(t) - \frac{P_L(t)}{\eta_D}u_3(t) + \eta_C[P_{pv}(t)u_1(t) + P_G(t)u_2(t)], \quad (12)$$

where $t = 0, 1, \dots, T-1$; $u_1(t)$, $u_2(t)$ and $u_3(t)$ are on-off status of switches U_1 , U_1 and U_3 over $[t-1, t)$. $P_{pv}(t)$ is the power of PV for charging the battery when $u_1(t) = 1$; $P_G(t)$ is the power of grid for charging the battery when $u_2(t) = 1$; $P_L(t)$ is the load demand discharged from the battery when $u_3(t) = 1$. According to Eq. (12), the current SOC $S(t)$ can be expressed by the initial SOC $S(0)$ of a day as

$$S(t) = S(0) - \sum_{\tau=0}^{t-1} \frac{P_L(\tau)}{\eta_D}u_3(\tau) + \eta_C \sum_{\tau=0}^{t-1} [P_{pv}(\tau)u_1(\tau) + P_G(\tau)u_2(\tau)]. \quad (13)$$

Note that the battery SOC of PDB system is decided by the power flows as Eq. (4), but the battery SOC of switching PV system is decided by the switching variables as Eq. (12).

3.4. Control system model

Using the switching PV system, the electricity cost over the period $[0, T)$ can be formulated as

$$\int_{\tau=0}^T \rho(\tau)[P_G(\tau)u_2(\tau) + P_L(\tau)u_4(\tau)]d\tau, \quad (14)$$

where $P_G(\tau)u_2(\tau)$ is the grid power consumed by the battery and $P_L(\tau)u_4(\tau)$ is the grid power consumed by the load.

In the approach of control, the switching grid-connected PV system is firstly modeled as a multiple-input and single-output (MISO) control system. In the PV system, the inputs include the on-off status of switches, and the output is the electricity cost. Denote the binary control input as $u(t) \triangleq [u_1(t), u_2(t), u_3(t), u_4(t), u_5(t)]^T$, and the state as $x(t) \triangleq S(t)$. The control output $y(t)$ is the electricity cost over $[t, t+1)$. According to SOC dynamic Eq. (12), the MISO linear state-space equation can be expressed as

$$\begin{cases} x(t+1) = x(t) + B(t)u(t), \\ y(t) = D(t)u(t), \end{cases} \quad (15)$$

where the input matrix $B(t)$ and the feed-forward matrix $D(t)$ are time varying. They are formulated as

$$\begin{cases} B(t) = [\eta_C P_{pv}(t), \eta_C P_G(t), -\frac{P_L(t)}{\eta_D}, 0, 0], \\ D(t) = [0, \rho(t)P_G(t), 0, \rho(t)P_L(t), 0]. \end{cases} \quad (16)$$

4. Control methodology

Modern control techniques can be applied on the proposed control system model. For any kind of control method, it is necessary to satisfy certain operational conditions. For the switching PV system, the control input $u(t)$ and the state $S(t)$ ($0 \leq t < T$) have several constraints:

- (i) PV output constraint: The PV's power is either used for charging battery or used for customers' consumption. In other words, the switches U_1 and U_5 cannot be on at the same time.

$$u_1(t) + u_5(t) \leq 1. \quad (17)$$

- (ii) Demand balance constraint: Because multiple power supply is not supported in the switching system, load demand of customers must be exactly satisfied by one of the three sources, i.e., the PV's power, the grid power and the battery power. Among the switches U_3 , U_4 and U_5 , only one can be on at each hour.

$$\begin{cases} u_3(t) + u_4(t) + u_5(t) = 1, \\ P_L(t)[u_3(t) + u_4(t)] + P_{pv}(t)u_5(t) \geq P_L(t), \end{cases} \quad (18)$$

(iii) Charging and discharging constraint: For safety and other physical reasons, the battery is not allowed for charging and discharging at the same time, and it cannot be charged by the PV and grid at the same time. In other words, the switches U_1 , U_2 and U_3 can only have one of them switched on at each hour.

$$u_1(t) + u_2(t) + u_3(t) = 1. \quad (19)$$

(iv) SOC boundary constraint: The SOC of battery must be less than the battery's capacity S^{max} and larger than the minimal allowable value S^{min}

$$S^{min} \leq S(t) \leq S^{max}. \quad (20)$$

(v) SOC terminate state constraint: For the convenience of dispatching power over the following day, the power of battery should not be used out till the initial value of SOC is reached. In this model, the terminate SOC of battery must be no less than the initial SOC as

$$S(0) \leq S(T). \quad (21)$$

In this paper, the optimal switching control is proposed to economically schedule the PV system. Besides the optimal control, an intuitive control method is also designed for comparison studies. Both these two control methods are employed for the PV system control in this paper.

4.1. Intuitive control

The intuitive switching control is designed to intuitively satisfy constraints (i–iv). The intuitive control is a rule-based method, in which the solar power has the highest priority of usage. The solar power is employed for satisfying the load demand or charging the battery. If the load demand cannot be satisfied by the solar power, the grid power is used. If the batter has low SOC, the grid power is also used to charge the battery. This intuitive method is sufficiently use solar energy for reducing the electricity cost. For time t , the control input is decided as the following steps:

- (a) If $P_L(t) \leq P_{pv}(t)$, $u_1(t) = 0$, $u_3(t) = 0$, $u_4(t) = 0$, $u_5(t) = 1$. In this case, if $S(t) \leq 1.25S^{min}$, $u_2(t) = 1$, otherwise $u_2(t) = 0$.
- (b) If $P_L(t) > P_{pv}(t)$ and $S(t) > 0.9S^{max}$, $u_1(t) = 0$, $u_2(t) = 0$, $u_3(t) = 1$, $u_4(t) = 0$, $u_5(t) = 0$.
- (c) If $P_L(t) > P_{pv}(t)$ and $1.25S^{min} < S(t-1) \leq 0.9S^{max}$, $u_1(t) = 1$, $u_2(t) = 0$, $u_3(t) = 0$, $u_4(t) = 1$, $u_5(t) = 0$.
- (d) If $P_L(t) > P_{pv}(t)$ and $S(t) \leq 1.25S^{min}$, $u_1(t) = 0$, $u_2(t) = 1$, $u_3(t) = 0$, $u_4(t) = 1$, $u_5(t) = 0$.

4.2. Optimal control

Optimal control of the evaluated PV system aims to minimize the electricity cost under TOU. Given the profiles

of PV output and load demand, the electricity cost over the period $[0, T)$, can be expressed by the control input according to Eqs. (14) and (15). The electricity cost can be regarded as the objective function in the optimal control. Considering constraints (i–v), the optimal control approach for the PV system is to find the optimal solution of the objective function that can be expressed as

$$J = \sum_{t=0}^{T-1} y(t) = \sum_{t=0}^{T-1} D(t)u(t), \quad (22)$$

$$s.t. \begin{cases} u_1(t) + u_5(t) \leq 1, \\ u_3(t) + u_4(t) + u_5(t) = 1, \\ P_L(t)[u_3(t) + u_4(t) - 1], \\ +P_{pv}(t)u_5(t) \geq 0, \\ u_1(t) + u_2(t) + u_3(t) = 1, \\ S^{min} \leq S(t) \leq S^{max}, \\ S(0) \leq S(T), \end{cases}$$

where $y(t)$ is the hourly electricity cost calculated in Eq. (15).

It can be noticed that the above optimal control problem is a linear programming problem with binary variables. Let U denote the decision vector $[u^T(0), u^T(1), \dots, u^T(T-1)]^T$, and f denote the coefficient vector $[D(0), D(1), \dots, D(T-1)]$. Then the optimal control problem can be converted into a standard form of linear programming as

$$J = fU, \quad (23)$$

$$s.t. \begin{cases} A_{ine}U \leq b_{ieq}, \\ A_{eq}U = b_{eq}, \end{cases}$$

where the first part of constraint set includes all equality constraints and the second part includes all inequality constraints. A_{ine} , b_{ine} , A_{eq} and b_{eq} can be easily deduced, so the explicit details are omitted here.

As the operation of PV system has constraints (i–v), the optimal control approach is a suitable method to satisfy these constraints while minimizing the electricity cost. Note that the intuitive method is a rule based method that can hardly ensure all constraints satisfied. The optimal control can achieve the lower cost that other control methods, but in the optimal control certain prerequisites must be ensured that load demand and PV output are predicted accurately over the control horizon $[0, T)$.

5. Experimental results

The switching PV system in this paper is a modification of the PDB system mentioned in Tazvinga et al. (2013) and Zhu et al. (2014). The sizing of PV and battery bank capacity is properly designed based on a sizing model in Hove and Tazvinga (2012). Note that other complicated methods on the level of system design, such as economic analysis and optimal sizing (Yang et al., 2009; Roy et al., 2010), can be considered for new installations of the switching PV system. As the scope here is on the operation level to

discuss how to schedule the installed PV system with grid connection, these important issues on the level system design are neglected in our discussion.

Configuration of the PV system is introduced here. The battery bank consists of 4×4 LONGWAY lead-acid batteries, i.e., 4 batteries are serially connected as a set and 4 sets are connected in parallel. Each battery's parameter is 12 V, 150 Ah, so the nominal battery capacity is 28.8 kW h and voltage output is 48 V. The PV module consists of 14 PV TENESOL panels; each of them has the capacity 250 W. The MPPT controller is integrated in MICROCARE charger, and another AC/DC charger is employed for storage of the grid power. The FUSION DC/AC inverter has equipped with the nominal capacity 6 kW. The parameters of this system are listed in Table 1. Note that charge and discharge efficiencies are regarded as 85% and 100% in this paper for newly installed charger and inverter. During the lifetime, efficiencies may decrease due to system performance deterioration. This factor of decreased efficiencies will be discussed in the next section.

Profile forecast of load demand and PV output must be accurate in the optimal control approach. For this purpose, daily profiles of load demand and PV output can be forecast online using some short-term forecasting methods (Bacher et al., 2009; Mellit and Pavan, 2010; Suganthi and Samuel, 2012). Given daily forecast profiles, the optimal schedule can be obtained in our proposed approach. Due to length limit, the profile forecast methods are not particularly studied, as the focus of this paper is system modeling and verification. We refer the profiles of casual days during summer and winter respectively, which have been studied at the same rural community clinics in Zimbabwe Tazvinga et al. (2013), Zhu et al. (2014). The load profiles in the summer and winter are plotted in Fig. 3. The profiles of PV output in the summer and winter are shown in Fig. 4. Note that profiles of any short-term forecasting method can be used as parameters of the proposed model. The effects of forecasting errors will be discussed in the next section.

Given these profiles of PV power and load demand, optimal control as an open-loop control method will be utilized to schedule the hourly on–off status $u_i(t) (i = 1, \dots, 5)$ over a day to minimize the electricity bill as Eq. (22). In the objective function, the installation cost is not considered in the model, as the scope here is discussing how to operate the installed hybrid system in the running period. The

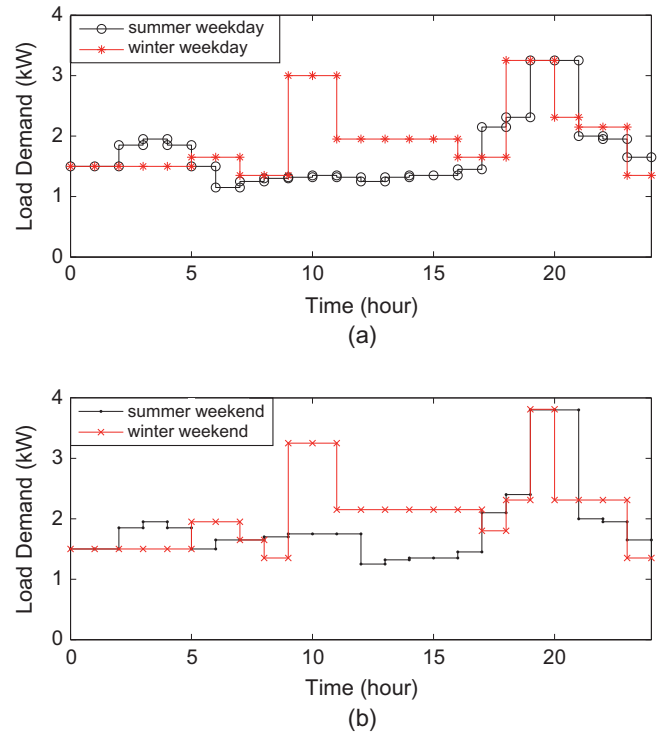


Fig. 3. Profiles of hourly load demand: (a) summer and winter weekdays; (b) summer and winter weekends.

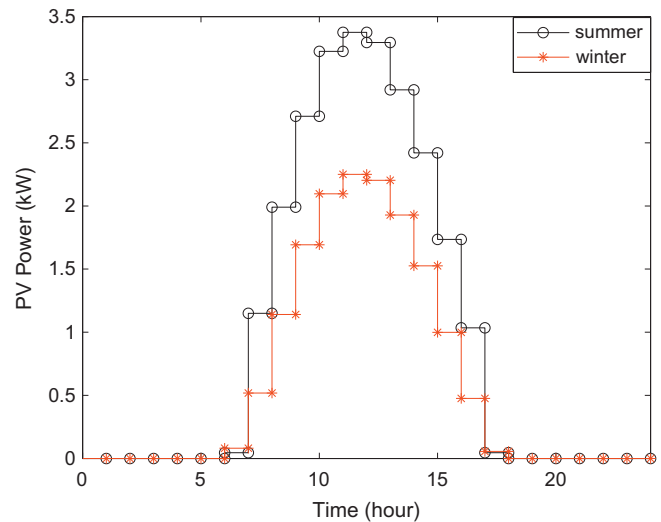


Fig. 4. Profiles of hourly PV power output.

Table 1
Parameters of PV–battery system.

Nominal battery capacity	28.8 kW h
Battery charging efficiency	85%
Battery discharging efficiency	100%
Battery's depth of discharge	40%
Initial state of charge	27 kW h
Hourly grid charge energy	4 kW h
PV array's capacity	3.5 kW

operation costs of PV and battery are also taken as negligible values for the period considered in the model.

As customers' daily demand changes between summer and winter, 4 cases will be evaluated, i.e., weekdays of summer and winter, weekends of summer and winter. An optimal switching solution will be found for each case. Because the decision variables are binary, i.e., 0 and 1, the linear binary programming method is used to solve the optimal control problem. For example, the *bintprog* function in MATLAB can solve such linear binary problem. In the

following simulation, the evaluation period is a day, i.e., $T = 24$. The electricity cost when only using the grid power is a baseline for the calculation of cost savings. It is uneasy to find similar methods of switching the hybrid system in literature, so the optimal switching method is compared with the intuitive method as introduced in Section 4.

- (1) Summer weekday: While only using the grid power, the electricity cost is \$3.493. By the intuitive method, the electricity cost is \$2.343. By optimal operation of hybrid system, the electricity bill is reduced to \$1.185. For a summer weekday, the optimal solution is plotted in Fig. 5. Over the peak period, the battery and the PV are employed for power supply. For example, the PV is employed over [8, 10) and the battery is employed over [18, 20). Over the off-peak period, the battery power is used to supply load demand firstly and then the battery is charged by the grid power. Over the peak PV output period [10, 14), the PV power are stored in the battery for later usage.
- (2) Summer weekend: While only using the grid power, the electricity bill is \$3.986. By the intuitive method, the electricity cost is \$2.616. By optimal operation of hybrid system, the electricity bill is reduced to \$1.310. Due to difference between load demand profiles, the optimal solution of a summer weekend is much different with that of a summer weekday as shown in Fig. 6. More grid power is used over the off-peak period [0, 7) instead of the battery power. Less PV power is stored in the battery for directly supplying load demand over the peak PV output period [10, 14).

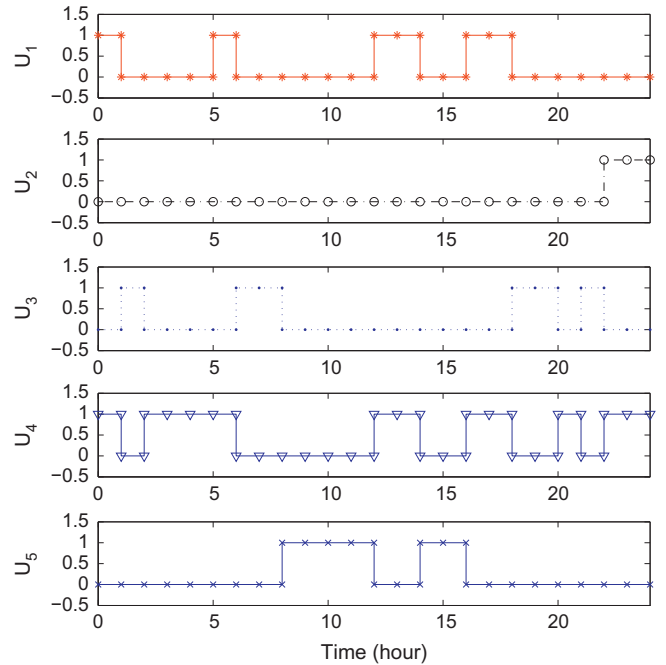


Fig. 6. Optimal switching operation in summer weekends.

- (3) Winter weekday: While only using the grid power, the electricity bill is \$4.274. By the intuitive method, the electricity cost is \$3.417. By optimal operation of hybrid system, the electricity bill is reduced to \$1.821. Different from summer weekdays, the grid power is used to supply load demand on most hours as shown in Fig. 7. Over the peak period the batter is discharged, and over the peak PV output period the PV power is used for direct power supply.

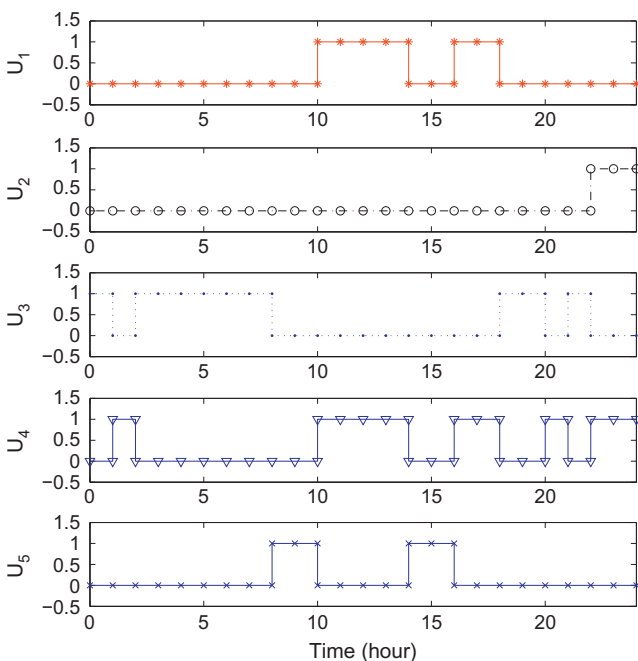


Fig. 5. Optimal switching operation in summer weekdays.

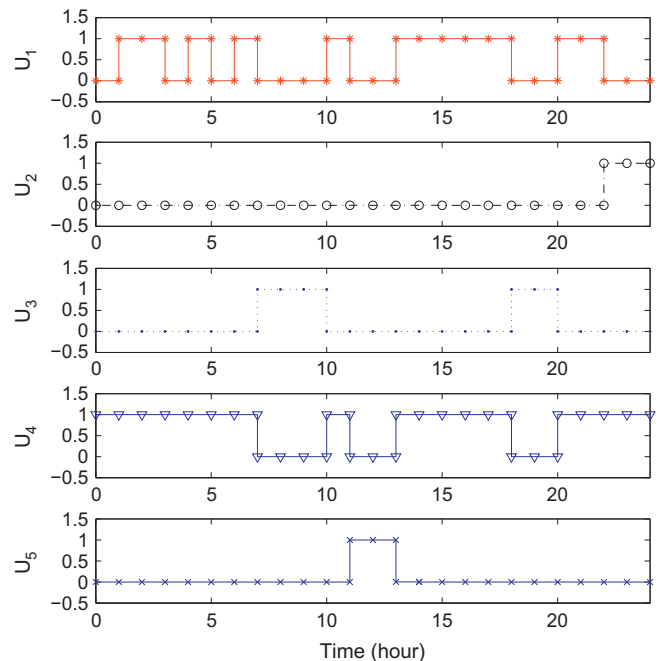


Fig. 7. Optimal switching operation in winter weekdays.

(4) Winter weekend: While only using the grid power, the electricity bill is \$4.465. By the intuitive method, the electricity cost is \$3.558. By optimal operation of hybrid system, the electricity bill is reduced to \$1.944. The similar observation can be drawn that the grid power is used to supply load demand on most hours as shown in Fig. 8. Besides the peak period, the battery is still discharged over [20, 21).

In all, the monthly bill (including 8 weekends and 22 weekdays) in summer is \$36.55 by the optimal switching approach, while the bill is \$72.47 by the intuitive method. The monthly bill in summer is \$56.61 by the optimal switching approach, while the bill is \$103.64 by the intuitive method. Hybrid systems can help customers to save electricity cost, and in the optimal approach larger cost saving can be achieved than the intuitive method.

6. Discussion

In the experimental studies, the battery initial SOC and the charging and discharging efficiency are fixed over a day period. In the life cycle of battery, these parameters must change year by year due to system deterioration. The effects of varying initial SOC, charging efficiency and discharging efficiency on the cost savings will be discussed in this section. Furthermore, forecasting errors of load demand and PV output may exist, so the effects of such errors on the control performance are also discussed. A summer weekday is chosen as an example day for the following discussion.

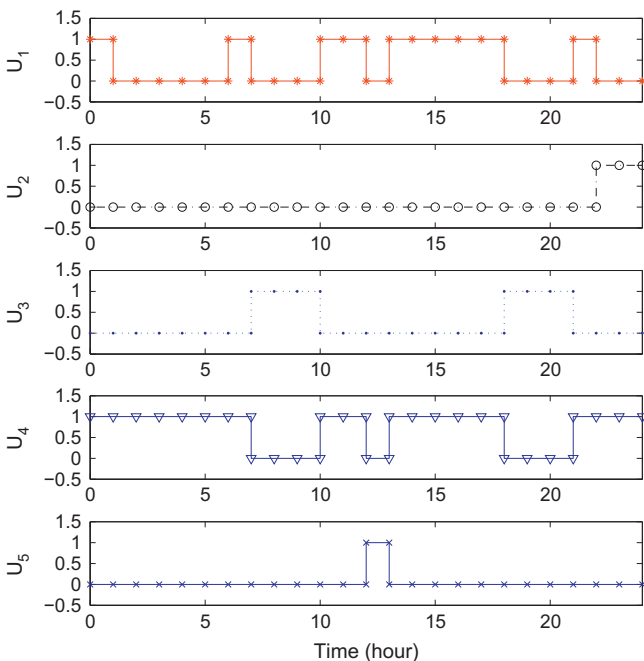


Fig. 8. Optimal switching operation in winter weekends.

6.1. Effects of initial SOC

In this kind of case studies, the initial SOC is set as 27 kW, 24 kW, 21 kW, 18 kW and 15 kW respectively. The other settings are kept the same as Table 1. Note that the charging and discharging efficiency is 85% and 100% respectively.

Under different initial SOC, the daily cost of switching PV system is given in Table 2. The observation is that low initial SOC introduces low electricity cost. The lower initial SOC is preferred for achieving larger cost savings. The possible reason is that the empty battery has enough capacity for charging over the peak PV output period as shown in Fig. 9. The figure indicates the profiles of SOC under these initial values. It can be noticed that the battery is charged and discharged with the same pattern. However, under low initial SOC the battery will be discharged toward the minimum requirement and then be charged sufficiently toward the maximum capacity.

6.2. Effects of charging efficiency

In this kind of case studies, the charging is set as 95%, 85%, 75% and 65% respectively. The other settings are kept the same as Table 1. Note that the initial SOC is 27 kWh and the discharging efficiency is 100%.

The daily cost of optimal switching control under different charging efficiency is calculated as given in Table 3. It can be observed that high charging efficiency can greatly reduce the electricity cost. When the old battery is

Table 2
Daily cost of different initial SOC.

SOC (kW h)	27	24	21	18	15
Cost (\$)	1.185	1.106	1.107	1.044	1.044

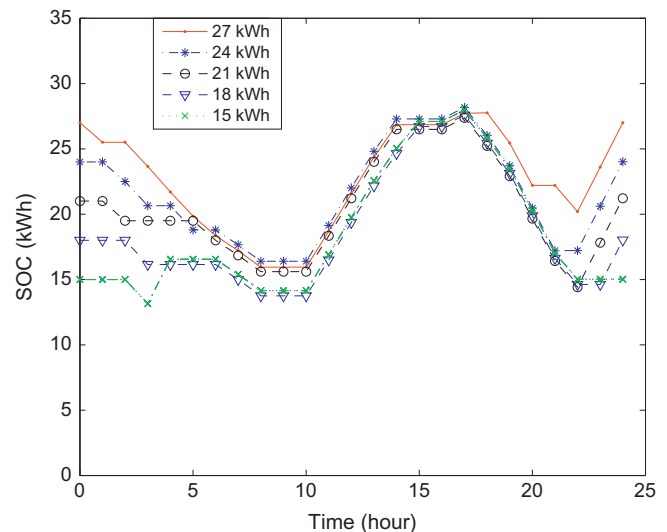


Fig. 9. Profiles of SOC with different initial values.

Table 3
Daily cost of different charging efficiencies.

η_C	95%	85%	75%	65%	55%
Cost (\$)	1.098%	1.185	1.263	1.375	1.443

Table 4
Daily cost of different discharging efficiencies.

η_D	100%	90%	80%	70%	60%
Cost (\$)	1.185	1.255	1.361	1.425	1.605

getting old, the daily cost is increasing. It is suggested to retrofit a new battery when the charging efficiency is lower than 70%.

6.3. Effects of discharging efficiency

In this kind of case studies, the discharging efficiency is set as 100%, 90%, 80%, 70% and 60% respectively. The other settings are kept the same as Table 1. Note that the initial SOC is 27 kW h and the charging efficiency is 85%.

The daily cost of optimal control under different discharging efficiency is given in Table 4. The observation of varying discharging efficiency is similar with charging efficiency. High discharging efficiency can introduce low electricity cost. When the battery gets old with relatively low discharging efficiency, the cost increases greatly. A new battery is suggested for retrofitting when the discharging efficiency is lower than 70%.

6.4. Effects of forecasting errors

Forecasting errors of load demand and solar power are often regarded as a standard probability distribution. For simplicity, the actual load demand is assumed as 110% of the forecasting load in the first case study; the actual solar power is assumed as 90% of the forecasting solar power in the second case study. Note that the electricity cost is \$1.185 if forecasting profiles are accurate.

In the first case, the electricity cost increases to \$1.275, because the actual load demand is larger than the forecasting one. It has been checked that the load forecasting error does not violate the demand balance constraint that is satisfied over the weekday.

In the second case, an interesting observation is that the electricity cost keeps the same as \$ 1.185. The cost does not change because less solar power output only brings less storage in the battery without any effect on the grid power consumption. The demand balance constraint is checked and is not violated by the solar forecasting error.

The SOC sensitivity on uncertain forecasting errors is analyzed as shown in Fig. 10. The errorless SOC is a baseline for the sensitivity analysis, and the boundary range [90%, 110%] is given as dotted lines in the figure. In these case studies, load and solar forecasting errors cause variations of SOC as shown in the figure. The load error

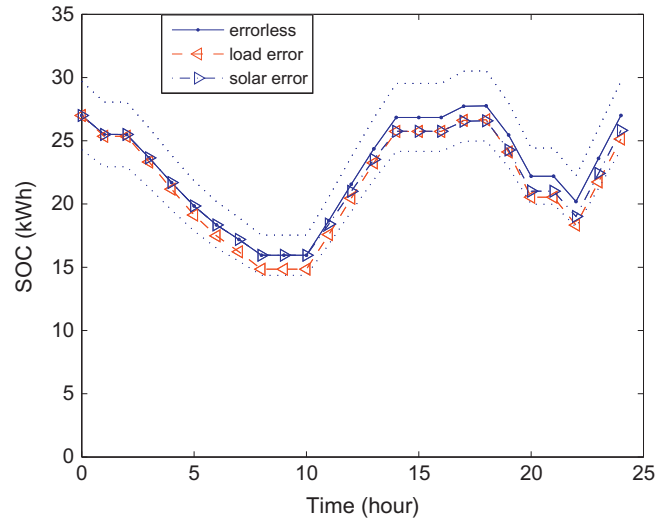


Fig. 10. SOC sensitivity on forecasting errors.

introduces larger variation than the solar error, because the actual load demand asks for more discharging power from the battery. It can also be noticed that the SOC variations lie in the boundary range. Therefore, the proposed optimal control approach has good robustness when the forecasting errors are smaller than 10%. The common weakness of open loop control methods is their disability on extremely large parameter errors, which is the same situation in the optimal control.

7. Conclusion

Grid-connected PV system with storage has been studied in the approach of optimal switching control. The resulted schedule of the PV system is expected to optimally integrate the solar energy into DSM. As an example of demand side program, time of use has been evaluated in the optimal switching control for reducing the electricity cost of customers. In the PV system, connections between each pair of components are controlled by switches. The power flow in each line depends on the number of on switches, as a result no additional adaptor and regulator is required in the switching control. The construction cost of switching system is much less than that of power flow control system with expensive regulators.

Under the TOU program, the electricity cost has been modeled in terms of switching status and electricity price under practical constraints, such as demand balance and PV output. The optimal solution to the model has made the best use of solar energy to charge the battery in the off-peak hours and discharge it in the peak hours. The results obtained indicate that the electricity cost has been largely reduced by the optimal switching control.

The optimal switching control is compared with an intuitive control method. The monthly electricity bill reduces to about 50% by the optimal approach. System parameters, such as initial SOC, forecast profiles, charging and discharging efficiencies has influences on the control

performance. As discussed, the proposed approach has good robustness for handling different kinds of parameter variations. By the optimal operation, people consume the minimal electricity and achieve great cost savings when the PV system has fixed or uncertain parameters.

The optimal switching control is a useful open-loop control method to schedule switching status of each line for satisfying practical constraints. Optimal control cannot handle the control task when the switching system suffers from extreme disturbances on PV output and load demand. In future work, the closed-loop control methods will be possibly developed to cope with such uncertain disturbances. Note that wind turbines or hydrokinetic generators may be integrated by parallel connections with PV generators for multiple power supply. The PV system is studied as it is commonly used in some areas where there is a lack of wind and water resources. Other future work is to extend our model to fit more complicated systems that consist of wind power, hydrokinetic power, biomass power and other renewable resources.

References

- Aalami, H., Moghaddam, M.P., Yousefi, G., 2010. Demand response modeling considering interruptible/curtailable loads and capacity market programs. *Appl. Energy* 87 (1), 243–250.
- Arun, P., Banerjee, R., Bandyopadhyay, S., 2009. Optimum sizing of photovoltaic battery systems incorporating uncertainty through design space approach. *Sol. Energy* 83 (7), 1013–1025.
- Bacher, P., Madsen, H., Nielsen, H.A., 2009. Online short-term solar power forecasting. *Sol. Energy* 83 (10), 1772–1783.
- Collares-Pereira, M., Rabl, A., 1979. The average distribution of solar radiation correlation between diffuse and hemispherical and between daily and hourly insolation values. *Sol. Energy* 22, 155–164.
- Esen, M., Yuksel, T., 2013. Experimental evaluation of using various renewable energy sources for heating a greenhouse. *Energy Build.* 65, 340–351.
- Esen, H., Inalli, M., Esen, M., 2006. Technoeconomic appraisal of a ground source heat pump system for a heating season in eastern Turkey. *Energy Convers. Manage.* 47 (9), 1281–1297.
- Esen, H., Inalli, M., Esen, M., 2007. A techno-economic comparison of ground-coupled and air-coupled heat pump system for space cooling. *Build. Environ.* 42 (5), 1955–1965.
- Gabash, A., Li, P., 2013. Flexible optimal operation of battery storage systems for energy supply networks. *IEEE Trans. Power Syst.* 28 (3), 2788–2797.
- Hove, T., Tazvinga, H., 2012. A techno-economic model for optimising component sizing and energy dispatch strategy for PV–diesel–battery hybrid power systems. *J. Energy Southern Africa* 23 (4), 18–28.
- Jain, S., Agarwal, V., 2008. An integrated hybrid power supply for distributed generation applications fed by nonconventional energy sources. *IEEE Trans. Energy Convers.* 23 (2), 622–631.
- Kanchev, H., Lu, D., Colas, F., Lazarov, V., Francois, B., 2011. Energy management and operational planning of a microgrid with a PV-based active generator for smart grid applications. *IEEE Trans. Ind. Electron.* 58 (10), 4583–4592.
- Mellit, A., Pavan, A.M., 2010. A 24-h forecast of solar irradiance using artificial neural network: application for performance prediction of a grid-connected PV plant at Trieste, Italy. *Sol. Energy* 84 (5), 807–821.
- Nema, P., Nema, R., Rangnekar, S., 2009. A current and future state of art development of hybrid energy system using wind and PV-solar: a review. *Renew. Sustain. Energy Rev.* 13 (8), 2096–2103.
- Penangsang, O., Sulistijono, P., Suyantoro, 2014. Optimal power flow using multi-objective genetic algorithm to minimize generation emission and operational cost in micro-grid. *Int. J. Smart Grid Clean Energy* 3 (4), 410–416.
- Riffonneau, Y., Bacha, S., Barruel, F., Ploix, S., 2011. Optimal power flow management for grid connected PV systems with batteries. *IEEE Trans. Sustain. Energy* 2 (3), 309–320.
- Roy, A., Kedare, S.B., Bandyopadhyay, S., 2010. Optimum sizing of wind–battery systems incorporating resource uncertainty. *Appl. Energy* 87 (8), 2712–2727.
- Shaahid, S., El-Amin, I., 2009. Techno-economic evaluation of off-grid hybrid photovoltaic–diesel–battery power systems for rural electrification in Saudi Arabia—a way forward for sustainable development. *Renew. Sustain. Energy Rev.* 13 (3), 625–633.
- Soto, W.D., Klein, S., Beckman, W., 2006. Improvement and validation of a model for photovoltaic array performance. *Sol. Energy* 80 (1), 78–88.
- Suganthi, L., Samuel, A.A., 2012. Energy models for demand forecasting – a review. *Renew. Sustain. Energy Rev.* 16 (2), 1223–1240.
- Tazvinga, H., Xia, X., Zhang, J., 2013. Minimum cost solution to photovoltaic–diesel–battery hybrid power systems for remote consumers. *Sol. Energy* 96, 292–299.
- Tazvinga, H., Zhu, B., Xia, X., 2014. Energy dispatch strategy for a photovoltaic–wind–diesel–battery hybrid power system. *Sol. Energy* 108, 412–420.
- Tazvinga, H., Zhu, B., Xia, X., in press. Optimal power flow management for distributed energy resources with batteries. *Energy Convers. Manage.*
- Teleke, S., Baran, M., Bhattacharya, S., Huang, A., 2010. Rule-based control of battery energy storage for dispatching intermittent renewable sources. *IEEE Trans. Sustain. Energy* 1 (3), 117–124.
- Wang, C., Nehrir, M., 2008. Power management of a stand-alone wind/photovoltaic/fuel cell energy system. *IEEE Trans. Energy Convers.* 23 (3), 957–967.
- Wies, R., Johnson, R., Agrawal, A., Chubb, T., 2005. Simulink model for economic analysis and environmental impacts of a PV with diesel–battery system for remote villages. *IEEE Trans. Power Syst.* 20 (2), 692–700.
- Wu, Z., Xia, X., Wang, B., 2015. Improving building energy efficiency by multiobjective neighborhood field optimization. *Energy Build.* 87, 45–56.
- Yang, H., Wei, Z., Chengzhi, L., 2009. Optimal design and techno-economic analysis of a hybrid solar–wind power generation system. *Appl. Energy* 86 (2), 163–169.
- Zhu, B., Tazvinga, H., Xia, X., 2014. Switched model predictive control for energy dispatching of a photovoltaic–diesel–battery hybrid power system. *IEEE Trans. Control Syst. Technol.* <http://dx.doi.org/10.1109/TCST.2014.2361800>.